spectrum of laser produced plasma of various targets such as Ti, Cu, Zn, Ga, As, Zr, and Mo. Fig.L.7.1 shows the x-ray spectrum of titanium. The K-α (4.5 keV) and K-β (4.9 keV) lines, along with continuum emission, can be clearly seen. It also shows the spectrum of stainless steel (SS). The K-α lines of Cr (5.4 keV), Fe (6.4 keV) and Ni (7.5 keV) (constituents of SS) can be seen.

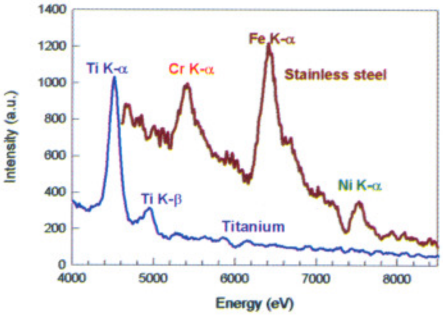

Fig. L.7.1: X-ray spectrum of Ti and stainless steel in the energy range around the inner shell transitions.

Under the same experimental conditions, the FWHM of the histogram of a dark frame was ~ 10 counts, resulting in a lower limit on the energy resolution of the spectrograph as ~ 67 eV. The energy resolution from the ionization statistics is ~ 109 eV. Thus, the overall resolution is expected to be ~ 128 eV. The FWHM of the Ti K-α line radiation (Fig.L.6.1) is measured to be ~ 136 eV, which is in close agreement with the theoretically expected resolution. Fig.L.7.2 shows the plot of photon energy as a function of CCD count. The plot shows a linear response with the photon energy in the whole spectral range. The X-intercept is due to the noise which gives a background count of ~ 270. The slope gives a calibration factor of ~ 6.78 [i.e.: Energy = 6.78 * (Counts - 270) eV] .The upper and lower limits on the spectral range of detection come from the CCD depletion region depth and the background counts respectively.

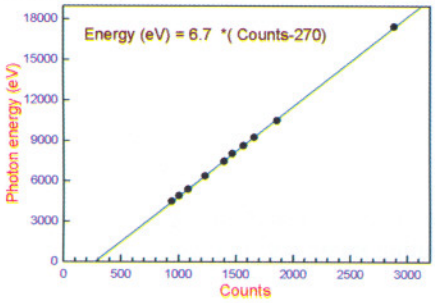

Fig. L.7.2: Calibration of the spectrograph in the 4 - 18 keV spectral range.

Reported by :
V.Arora (arora@rrcat.gov.in) and P.A.Naik

L.8: Pre-welding laser surface treatment to enhance inter-granular corrosion resistance of gas tungsten arc weldment of type 304 stainless steel

A novel pre-welding laser surface treatment has been developed by Laser Material Processing Division of RRCAT for gas tungsten arc welding (GTAW) of austenitic stainless steel, to effectively enhance its resistance against heat-affected zone (HAZ) sensitization and inter-granular corrosion (IGC). During welding of austenitic stainless steels, particularly of high carbon content, HAZ of the weldment gets sensitized, which adversely affects its resistance against IGC during its service in susceptible environment. The phenomenon is referred as "weld decay". IGC of austenitic stainless steel arises from inter-granular precipitation of chromium-rich carbides in the temperature range of 773 - 1073 K. Inter-granular carbide precipitation is accompanied by the development of chromium-depleted zone adjacent to grain boundaries. Chromium-depleted zones, being anodic with respect to grain interior, are preferentially attacked in the corrosive environment leading to IGC. This state is referred as "sensitization". IGC is one of the major problems experienced by welded components of austenitic stainless steel, operating in process industry.

The present study was performed on 6 mm thick medium carbon (0.044 wt %) and 10 mm thick high carbon (0.1 wt %) sheets of type 304 stainless steel. Laser surface treatment was performed with an indigenously developed 4 kW CO_2 laser operated in pulse-periodic mode. The results of the experimental study established that surface modification induced by pre-weld CO_2 laser treatment is highly effective in suppressing HAZ-sensitization during subsequent gas tungsten arc welding. Laser surface treated HAZ of gas tungsten arc weldment exhibited significantly lower degree of sensitization and susceptibility to IGC than those of untreated HAZ. The degree of sensitization of untreated and laser surface treated HAZ specimens, as determined by double-loop electro-chemical potentio-kinetic reactivation (DL-EPR) test, are summarized in Table L.4.1. Enclosed figure (see Fig. L.8.1) compares untreated HAZ (marked as "N-HAZ") and pre-weld laser treated HAZ (marked as "LSM-HAZ") specimens of high carbon variety of stainless steel after undergoing IGC test, as per ASTM A262 practice E. It can be noticed from this figure that IGC tested untreated HAZ specimen broke into two pieces whereas pre-weld laser surface treated HAZ specimen remained uncracked.

Table L.8.1 : Results of DL-EPR Tests

Specimen		% Degree of sensitization (DOS)	
		Top surface	**Bottom surface**
Medium C type 304 SS	Untreated HAZ	0.45	0.26
	Laser treated HAZ	0.0123	-
High C type 304 SS	Untreated HAZ	12.38	42
	Laser treated HAZ	0.031	0.029

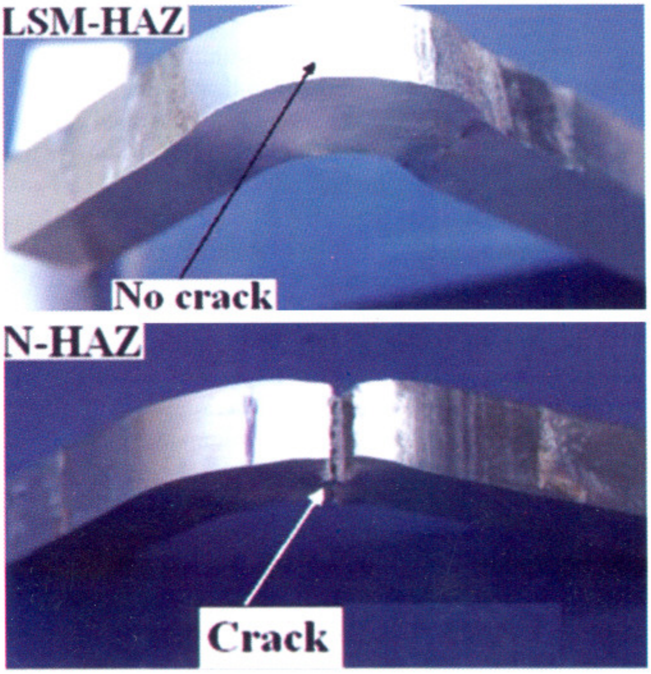

Fig. L.8.1: Comparison of untreated HAZ (N-HAZ) and pre-weld laser treated HAZ (LSM-HAZ) specimens of type 304 stainless steel after undergoing IGC test - ASTM A262 Practice E.

The pre-welding laser surface treatment technique has a strong potential in enhancing life of austenitic stainless steel welded components operating in corrosive environment, especially prevalent in process industry. This study has been performed in collaboration with Corrosion Science & Technology Division of Indira Gandhi Centre for Atomic Research, Kalpakkam.

Reported by:
R. Kaul (rkaul@rrcat.gov.in), and L. M. Kukreja

L.9: Dependence of the high order harmonic intensity on the length of the plasma plume

High order harmonic generation from the interaction of ultra-short laser pulses with a gaseous medium is an attractive method of generating ultra-short coherent XUV radiation. It is desirable to have high intensity of the harmonics for their deployment in practical applications. In this regard, the use of weakly ionized under-dense plasma plume as the medium for harmonic conversion has an interesting possibility of resonant intensity enhancement of particular harmonic orders. One may also achieve high harmonic intensity by increasing the medium length. However, phase mismatch between the laser field and the harmonic radiation due to medium dispersion accumulated during propagation over large medium length may limit the growth of harmonic intensity. Laser Plasma Division of RRCAT has carried out an experimental study on the variation of harmonic intensity with medium length in low ionized laser produced plasma plumes.

The laser used in the study was a 10 Hz Ti:sapphire laser ($\lambda = 790$ nm). A part of the uncompressed laser pre-pulse of duration ~300 ps was line focussed by two crossed cylindrical lenses on a planar silver strip of 2 mm width, to a focal-spot size of 2 mm x300 µm. After a delay of 60 ns, the main laser pulse ($\tau \sim 45$ fs) was focussed in the plasma plume, with the beam propagating parallel to target surface. The peak laser intensity of the fs pulse at the centre of the plasma plume was ~2.5 10^{15} W/cm^2. To study the effect of medium length on harmonic emission, the length of the plasma plume was varied (in the range of 0.8 mm to 2 mm) by inserting a slit of variable width in the centre of the pre-pulse beam before the lens assembly. The high-order harmonics were analyzed by an in-house developed flat-field grazing-incidence spectrograph, and were detected by an MCP-CCD camera combination. The odd harmonics up to 47th harmonic order were observed.

The variation of the 21st, 33rd and 41st harmonic intensity with plasma plume length is shown in Fig.L.9.1. It is seen from the figure that the intensity of harmonics (I_H) increases with the medium length (L_{med}) as $I_H \quad (L_{med})^{\beta}$, where the scaling exponent β is ~ 0.9, 0.8, and 0.7 for 21st, 33rd, and 41st harmonics respectively. Next, the variation of harmonic intensity with harmonic order for two different plume lengths is shown in Fig.L.9.2. It is seen from this figure that the harmonic intensity decreases with increasing harmonic order, which is in variance with the plateau-like behaviour observed in gaseous media.